Available online at www.sciencedirect.com
SCIENCE DIRECT®
Computers and Structures 82 (2004) 2341–2350
Computers & Structures
www.elsevier.com/locate/compstruc

# New control strategies for active tuned mass damper systems

H. Cao [a], Q.S. Li [b,*]

[a] Department of Transportation, California, USA
[b] Department of Building and Construction, City University of Hong Kong, Kowloon, Hong Kong

Received 12 June 2003; accepted 12 May 2004
Available online 3 July 2004

**Abstract**

A different structural control approach is developed in this paper. Instead of solving the Riccati equation, new active control strategies are proposed from a response parameter analysis for the design of active tuned mass damper (ATMD) systems. A simplified method for ATMD design is presented based on the proposed strategies. As a main feature, the equivalent damping induced by an ATMD can be determined by the simplified method. In order to examine the performance of the proposed formulas and the active control strategies, numerical simulations are carried out for some examples. The numerical results show that the present strategies result in a better reduction on acceleration response than the linear quadratic regulator (LQR) method. It is also shown through numerical examples that the results determined from the simplified design method are close to those obtained from the present strategies and the LQR method.


*Keywords:* Structural control; Tuned mass damper; Vibration; High-rise structure

## 1. Introduction

The most commonly used active control device for civil engineering structures is the active tuned mass damper (ATMD). As Li et al. [11] commented, the high efficiency is the major advantage of ATMD, in which a relatively small mass can be used to reduce structural response. Meanwhile an active control force is applied to move this small mass efficiently in order to achieve further response reduction. Thus, a relatively small active control force can significantly reduce structural response by 40–50% or more [2]. On the other hand, unlike some other active control devices, ATMD can be installed in many kinds of structures: buildings, towers and bridges.

Three kinds of ATMDs have been developed over the last two decades. They are the hybrid mass damper (HMD), the active mass damper (AMD) and DUOX (Figs. 1 and 2). A significant difference between a HMD and an AMD is that the stiffness and damping of HMD are provided by a tuned mass damper, while the stiffness or/and damping of an AMD is provided by the active force [13]. The so-called "DUOX" system is composed of three parts, a small mass, a tuned mass damper and an active force [2]. The active force, mainly used to reduce the stroke of the TMD in the DUOX system, is applied to the TMD through the action of the small mass (see Fig. 2).

Extensive theoretical and experimental studies on AMD devices have been conducted by many researchers e.g., [1–8,12–14,16]. The first practical application of an AMD device in the world was realized in Japan in 1989, when two AMDs were installed on the 11th floor of a commercial office building, Kyobashi Seiwa Building in Tokyo by Kajima Cooperation. The objective of installing the AMDs is to control the lateral and torsional vibration of the building subjected to earthquakes and frequent strong winds. Since then, the active tuned mass dampers have been installed in several buildings, towers and bridges [3].

* Corresponding author.
*E-mail address:* bcqsli@cityu.edu.hk (Q.S. Li).

0045-7949/$ - see front matter © 2004 Elsevier Ltd. All rights reserved.
doi:10.1016/j.compstruc.2004.05.010

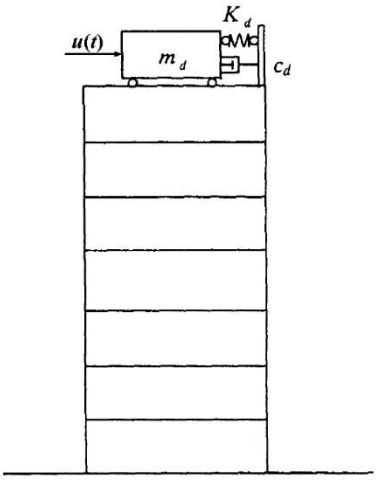


Fig. 1. HMD/AMD system.

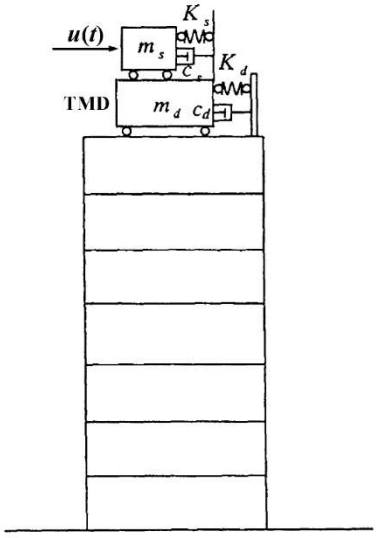


Fig. 2. DUOX system.

As is well known, all active structural control strategies are rooted in the modern control theory. The simplest and most popular strategy is the linear quadratic regulator (LQR) method. However, an active control strategy for an ATMD has its own specifications and limitations. Cao [2] has shown that highly nonlinear control strategies, such as bang–bang control, may not be suitable for ATMD applications. New control strategies, which are based on linear feedback control, are proposed in this paper from a response parameter analysis. Unlike the traditional LQR method, the new strategies do not need to solve the Riccati equation. Furthermore, a simplified method for ATMD design is presented based on the proposed strategies. As a main feature, the equivalent damping induced by an ATMD can be easily determined by the simplified method. In order to check the effectiveness of the proposed formulas and the active control strategies, numerical simulations are conducted for three examples. The numerical results show that the present strategies result in a better reduction on structural acceleration responses than the LQR method. It is also observed from the numerical examples that the results determined from the simplified design method are in good agreement with those obtained from the present strategies and the LQR method.

## 2. Equations of motion

As introduced above, a DUOX system is composed of three parts, a small mass, a tuned mass damper and an active force, as shown in Fig. 2. The equations of motion of a structure with a DUOX system under wind action can be expressed as

$$[M]\{\ddot{X}\} + [C]\{\dot{X}\} + [K]\{X\} = \{w(t)\} - \{L\}(c_d\dot{x}_d + k_d x_d) \tag{1}$$

$$m_d\ddot{x}_d + c_d\dot{x}_d + k_d x_d = -m_d\{L\}^T\{\ddot{X}\} - u(t) + c_s\dot{x}_s + k_s x_s \tag{2}$$

$$m_s\ddot{x}_s + c_s\dot{x}_s + k_s x_s = u(t) - m_s\ddot{x}_d - m_s\{L\}^T\{\ddot{X}\} \tag{3}$$

where $\{X\}$, $x_d$ and $x_s$ are relative displacements with respect to the ground, structure and TMD, respectively; $m_s$, $c_s$, $K_s$ and $m_d$, $c_d$, $K_d$ are the mass, damping, stiffness of the small mass and TMD, respectively. $[M]$, $[C]$ and $[K]$ are the mass, damping and stiffness matrices of the main structure. $\{w(t)\}$ is the vector of wind load acting on the main structure. We assume that wind loads are acted on each floor and can be expressed as

$$\{w(t)\} = \{S_j\}v(t) \tag{4}$$

where $S_j$ is a parameter related to wind and structural characteristics at the $j$th floor, $v(t)$ is wind velocity at a reference height (10 m above ground in this paper).

$\{L\}$ is the location vector of the control device. $u(t)$ is the active force.

For a structure with an AMD/HMD system, we have

$$[M]\{\ddot{X}\} + [C]\{\dot{X}\} + [K]\{X\} = \{w(t)\} - \{L\}(c_d\dot{x}_d + k_d x_d - u(t)) \tag{5}$$

$$m_d\ddot{x}_d + c_d\dot{x}_d + k_d x_d = -m_d\{L\}^T\{\ddot{X}\} + u(t) \tag{6}$$

In this paper, we mainly discuss the design of AMD systems. Hence, Eqs. (5) and (6) are considered in the following part of this paper.

If only the first $m$ modes of the main structure are considered, according to the method of mode superposition, the displacement vector can be expressed as

$$\{X(t)\} = \sum_{j=1}^{m} \{\Phi\}_j y_j(t) \tag{7}$$

where $\{\Phi\}_j$ and $y_j(t)$ are the $j$th mode shape function and the $j$th generalized modal coordinate of the structure, respectively.

It is assumed that the damping of the structure is Rayleigh, then, the equations of the $j$th generalized modal coordinate and relative displacement of the AMD are obtained by substituting Eq. (7) into Eqs. (5) and (6) as follows:

$$\ddot{y}_j(t) + 2\xi_j\omega_j\dot{y}_j(t) + \omega_j^2 y_j(t) - \mu_j\Phi_{ij}\left[2\xi_d\omega_d\dot{x}_d(t) + \omega_d^2 x_d(t)\right] = \Lambda_j v(t) - \frac{u(t)}{\widehat{M}_j}, \quad j = 1,2,\ldots,m \tag{8}$$

$$\ddot{x}_d(t) + 2\xi_d\omega_d\dot{x}_d(t) + \omega_d^2 x_d(t) + \sum_{j=1}^{m}\phi_{ij}\ddot{y}_j(t) = \frac{u(t)}{m_d} \tag{9}$$

where

$$\widehat{M}_j = \sum_{i=1}^{n}\Phi_{ij}m_i, \quad \mu_j = \frac{m_d}{\widehat{M}_j}$$
$$\Lambda_j = \frac{1}{\widehat{M}_j}\sum_{i=1}^{n}\Phi_{ij}^2 S_i, \quad \omega_d^2 = \frac{k_d}{m_d}, \quad 2\xi_d\omega_d = \frac{c_d}{m_d} \tag{10}$$

in which $n$ is the number of floor of the building under consideration.

In general, the first mode shape is dominant in wind-induced vibration of a structure [9,10]. Thus, only the first mode shape is considered herein. Taking the value of the first mode shape function at the AMD location (the $i$th floor) as one ($\Phi_{i1} = 1$), then Eqs. (8) and (9) become

$$\ddot{y}_1(t) + 2\xi_1\omega_1\dot{y}_1(t) + \omega_1^2 y_1 - 2\mu_1\xi_d\omega_d\dot{x}_d - \mu_1\omega_d^2 x_d = \Lambda_1 v(t) - \frac{1}{\widehat{M}_1}u(t) \tag{11}$$

$$\ddot{y}_1 + \ddot{x}_d + 2\xi_d\omega_d\dot{x}_d + \omega_d^2 x_d = \frac{1}{m_d}u(t) \tag{12}$$

Based on the assumption of the linear feedback control, the active control force $u(t)$ is expressed as

$$u(t) = -\begin{bmatrix} g_1^* & g_2^* & g_3^* & g_4^* & g_5^* & g_6^* \end{bmatrix} \times \begin{bmatrix} y_1 & x_d & \dot{y}_1 & \dot{x}_d & \ddot{y}_1 & \ddot{x}_d \end{bmatrix}^T \tag{13}$$

where

$$\begin{bmatrix} g_1^* & g_2^* & g_3^* & g_4^* & g_5^* & g_6^* \end{bmatrix} = m_d\begin{bmatrix} \frac{g_1}{\mu_1}\omega_1^2 & g_2\omega_d^2 & 2\frac{g_3}{\mu_1}\xi_1\omega_1 & 2g_4\xi_d\omega_d & \frac{g_5}{\mu_1} & g_6 \end{bmatrix} \tag{14}$$

The physical meanings of these control gains $g_k$ ($k = 1 \sim 6$), are:

1. $g_1$, $g_2$ and $g_5$, $g_6$ represent additional stiffness and additional mass, respectively, induced by the ATMD, their values are much less than one, hence their effects on the natural frequencies of the main structure are not significant.
2. $g_3$ and $g_4$ are not negative values, i.e., no negative damping is induced, hence the response of the main structure is stable.

Multiplying Eq. (12) by $\mu_1$, adding to Eq. (11) and substituting Eq. (13) into Eq. (12) result in

$$(1+\mu_1)\ddot{y}_1 + 2\xi_1\omega_1\dot{y}_1 + \omega_1^2 y_1 + \mu_1\ddot{x}_d = \Lambda_1 v(t) \tag{15}$$

$$\left(1 + \frac{g_5}{\mu_1}\right)\ddot{y}_1 + (1+g_6)\ddot{x}_d + \frac{g_3}{\mu_1}2\xi_1\omega_1\dot{y}_1 + (1+g_4) \times 2\xi_d\omega_d\dot{x}_d + \frac{g_1}{\mu_1}\omega_1^2 y_1 + (1+g_2)\omega_d^2 x_d = 0 \tag{16}$$

Eqs. (15) and (16) can be written in the following matrix–vector form

$$[\overline{M}]\{\ddot{Y}(t)\} + [\overline{C}]\{\dot{Y}(t)\} + [\overline{K}]\{Y(t)\} = \{\overline{F}(t)\} \tag{17}$$

where

$$[\overline{M}] = \begin{bmatrix} 1+\mu_1 & \mu_1 \\ 1+\frac{g_5}{\mu_1} & 1+g_6 \end{bmatrix} \tag{18}$$

$$[\overline{C}] = \begin{bmatrix} 2\xi_1\omega_1 & 0 \\ 2\frac{g_3}{\mu_1}\xi_1\omega_1 & 2(1+g_4)\xi_d\omega_d \end{bmatrix} \tag{19}$$

$$[\overline{K}] = \begin{bmatrix} \omega_1^2 & 0 \\ \frac{g_1}{\mu_1}\omega_1^2 & (1+g_2)\omega_d^2 \end{bmatrix} \tag{20}$$

$$\{\overline{F}(t)\} = \begin{Bmatrix} \Lambda_1 \\ 0 \end{Bmatrix} v(t) \tag{21}$$

$$\{Y(t)\} = \begin{Bmatrix} y_1(t) \\ x_d(t) \end{Bmatrix} \tag{22}$$

## 3. Control strategy for harmonic excitations

It is assumed that wind-type harmonic excitations can be expressed as

$$v(t) = v_0 e^{i\omega t} \tag{23}$$

and the displacements of the main structure and ATMD are

$$y_1(t) = A e^{i(\omega t - \theta_1)}, \quad A > 0 \tag{24}$$

$$x_d(t) = B e^{i(\omega t - \theta_2)}, \quad B > 0 \tag{25}$$

Substituting Eqs. (23)–(25) into Eq. (15) and using their real parts and imaginary parts yield

$$A' \cos\theta_3 - \mu_1 \omega^2 B \cos\theta_2 = \Lambda_1 v_0 \tag{26}$$

$$A' \sin\theta_3 - \mu_1 \omega^2 B \sin\theta_2 = 0 \tag{27}$$

where

$$A' = \sqrt{\left[\omega_1^2 - (1+\mu_1)\omega^2\right]^2 + (2\xi_1\omega_1\omega)^2}A \tag{28}$$

$$\theta_3 = \theta_1 - \tan^{-1}\frac{2\xi_1\omega_1\omega}{\omega_1^2 - (1+\mu_1)\omega^2} \tag{29}$$

Similarly, applying Eqs. (23)–(25) to Eq. (16) leads to

$$\begin{aligned}&\left[\frac{g_1}{\mu_1}\omega_1^2 - \left(1+\frac{g_5}{\mu_1}\right)\omega^2\right]A\cos\theta_1 + \frac{g_3}{\mu_1}2\xi_1\omega_1\omega A\sin\theta_1 \\ &\quad = \left[(1+g_6)\omega^2 - (1+g_2)\omega_d^2\right]B\cos\theta_2 - (1+g_4) \\ &\qquad \times 2\xi_d\omega_d\omega B\sin\theta_2\end{aligned} \tag{30}$$

$$\begin{aligned}&-\left[\frac{g_1}{\mu_1}\omega_1^2 - \left(1+\frac{g_5}{\mu_1}\right)\omega^2\right]A\sin\theta_1 + \frac{g_3}{\mu_1}2\xi_1\omega_1\omega A\cos\theta_1 \\ &\quad = -\left[(1+g_6)\omega^2 - (1+g_2)\omega_d^2\right]B\sin\theta_2 \\ &\qquad - (1+g_4)2\xi_d\omega_d\omega B\cos\theta_2\end{aligned} \tag{31}$$

When displacement amplitudes of the main structure and ATMD, $A$ and $B$, are given, the phase angles $\theta_1$ and $\theta_2$ can be determined from Eqs. (26) and (27) as

$$\theta_2 = \cos^{-1} - \frac{\Lambda_1^2 v_0^2 + \mu_1^2\omega^4 B^2 - A'^2}{2\Lambda_1 v_0 \mu_1 \omega^2 B} \tag{32}$$

$$\theta_1 = \sin^{-1}\left(\frac{\mu_1\omega^2 B}{A'}\sin\theta_2\right) + \tan^{-1}\frac{2\xi_1\omega_1\omega}{\omega_1^2 - (1+\mu_1)\omega^2} \tag{33}$$

Then the control gains can be obtained from Eqs. (30) and (31). It is noted that when

$$\left|\Lambda_1 v_0 - \mu_1\omega^2 B\right| \leqslant A \tag{34}$$

$$\left|\Lambda_1 v_0 - A'\right| \leqslant \mu_1\omega^2 B \tag{35}$$

Eqs. (26) and (27) are thus solvable, which means that amplitude $A$ has a limiting value. Two conclusions can be drawn from Eqs. (30) and (31):

(1) If $g_1 \sim g_6$ are the control gains, then $ag_1 \sim ag_6$ ($a$ is a positive constant) can also be chosen as control gains.
(2) Four of the control gains ($g_1 \sim g_6$) are arbitrary, and only two of them have to be determined from Eqs. (30) and (31). This conclusion is drawn based on the assumption that the chosen control gains would not cause unstable response.

Eqs. (30) and (31) represent the complete feedback control strategy. It should be noted that the state feedback and the other linear feedback control strategies are included in this formulation as special cases. For example, for the state feedback control, $g_5 = g_6 = 0$ Eqs. (30) and (31) become

$$\begin{aligned}&\left(\frac{g_1}{\mu_1}\omega_1^2 - \omega^2\right)A\cos\theta_1 + \frac{g_3}{\mu_1}2\xi_1\omega_1\omega A\sin\theta_1 \\ &\quad = \left[\omega^2 - (1+g_2)\omega_d^2\right]B\cos\theta_2 - (1+g_4) \\ &\qquad \times 2\xi_d\omega_d\omega B\sin\theta_2\end{aligned} \tag{36}$$

$$\begin{aligned}&-\left(\frac{g_1}{\mu_1}\omega_1^2 - \omega^2\right)A\sin\theta_1 + \frac{g_3}{\mu_1}2\xi_1\omega_1\omega A\cos\theta_1 \\ &\quad = -\left[\omega^2 - (1+g_2)\omega_d^2\right]B\sin\theta_2 - (1+g_4) \\ &\qquad \times 2\xi_d\omega_d\omega B\cos\theta_2\end{aligned} \tag{37}$$

or

$$\begin{aligned}g_3 = \mu_1 &\\ &\times \frac{\left(\omega^2 - \frac{g_1}{\mu_1}\omega_1^2\right)A\cos(\theta_1-\theta_2) + \left[\omega^2 - (1+g_2)\omega_d^2\right]B}{2\xi_1\omega_1\omega A\sin(\theta_1-\theta_2)}\end{aligned} \tag{38}$$

$$\begin{aligned}g_4 = &\frac{\left(\omega^2 - \frac{g_1}{\mu_1}\omega_1^2\right)A + \left[\omega^2 - (1+g_2)\omega_d^2\right]B\cos(\theta_2-\theta_1)}{2\xi_d\omega_d\omega B\sin(\theta_2-\theta_1)} \\ &- 1\end{aligned} \tag{39}$$

Because $g_1$ and $g_2$ can be arbitrarily chosen, $g_3$ and $g_4$ can be determined from Eqs. (38) and (39).

In the case of velocity feedback control, $g_1$ and $g_2$ are zero, $g_5$ and $g_6$ can be arbitrarily chosen, then $g_3$ and $g_4$ can be found from Eqs. (30) and (31) as

$$\begin{aligned}g_3 = \mu_1 &\\ &\times \frac{\left(1+\frac{g_5}{\mu_1}\right)\omega^2 A\cos(\theta_1-\theta_2) + \left[(1+g_6)\omega^2 - \omega_d^2\right]B}{2\xi_1\omega_1\omega A\sin(\theta_1-\theta_2)}\end{aligned} \tag{40}$$

$$g_4 = \frac{\left(1+\frac{g_5}{\mu_1}\right)\omega^2 A + \left[(1+g_6)\omega^2 - \omega_d^2\right]B\cos(\theta_2-\theta_1)}{2\xi_1\omega_d\omega B\sin(\theta_2-\theta_1)} \tag{41}$$

If only displacements, velocities or accelerations are used as feedback, the corresponding control strategies can be deduced as follows:

1. Displacement feedback

$$g_1 = \frac{\mu_1}{\omega_1^2}\left[\omega^2 - \frac{2\xi_d\omega_d\omega B}{A\sin(\theta_2-\theta_1)}\right] \tag{42}$$

$$g_2 = \frac{\omega^2}{\omega_1^2} + 2\xi_d\frac{\omega}{\omega_d}\cos(\theta_2-\theta_1) - 1 \tag{43}$$

2. Velocity feedback

$$g_3 = \mu_1\frac{\omega^2 A\cos(\theta_1-\theta_2) + (\omega^2-\omega_d^2)B}{2\xi_1\omega_1\omega A\sin(\theta_1-\theta_2)} \tag{44}$$

$$g_4 = \frac{\omega^2 A + (\omega^2-\omega_d^2)B\cos(\theta_2-\theta_1)}{2\xi_d\omega_d\omega B\sin(\theta_1-\theta_2)} - 1 \tag{45}$$

3. Acceleration feedback

$$g_5 = \mu_1\left[\frac{2\xi_d\omega_d\omega B}{A\omega\sin(\theta_2-\theta_1)} - 1\right] \tag{46}$$

$$g_6 = \frac{\omega_d^2}{\omega^2} - 2\xi_d\frac{\omega_d}{\omega}\cos(\theta_2-\theta_1) - 1 \tag{47}$$

## 4. Control strategy for random excitations

It is well known that an increase in active control force does not necessarily mean an increase in ATMD effectiveness. Therefore, it is understandable that an optimal active control force should be determined. A new optimal control strategy based on the linear feedback control is presented in this section. Instead of using the traditional LQR method, in which the Riccati equation needs to be solved, we derive the optimal control gains from variance of displacement responses.

The frequency response function corresponding to Eq. (17) is

$$H(\omega) = \frac{1}{\Delta}[h_{ij}(\mathrm{i}\omega)] \tag{48}$$

where

$$\Delta = \left|(\mathrm{i}\omega)^2[\overline{M}] + \mathrm{i}\omega[\overline{C}] + [\overline{K}]\right| = \sum_{j=0}^{4} a_j(\mathrm{i}\omega)^j \tag{49}$$

$$h_{11}(\mathrm{i}\omega) = -(1+g_6)\omega^2 + 2(1+g_4)\xi_d\omega_d(\mathrm{i}\omega) + (1+g_2)\omega_d^2 \tag{50}$$

$$h_{12}(\mathrm{i}\omega) = \mu_1\omega^2 \tag{51}$$

$$h_{21}(\mathrm{i}\omega) = \left(1+\frac{g_5}{\mu_1}\right)\omega^2 - 2\frac{g_3}{\mu_1}\xi_1\omega_1(i\omega) - \frac{g_1}{\mu_1}\omega_1^2 \tag{52}$$

$$h_{22}(\mathrm{i}\omega) = -(1+\mu_1)\omega^2 + 2\xi_1\omega_1(\mathrm{i}\omega) + \omega_1^2 \tag{53}$$

$$a_0 = (1+g_2)\omega_1^2\omega_d^2 \tag{54}$$

$$a_1 = 2(1+g_4)\omega_1^2\xi_d\omega_d + 2(1+g_2)\xi_1\omega_1\omega_d^2 \tag{55}$$

$$a_2 = (1-g_1+g_6)\omega_1^2 + 4(1+g_4)\xi_1\omega_1\xi_d\omega_d + (1+\mu_1)\times(1+g_2)\omega_d^2 \tag{56}$$

$$a_3 = 2(1-g_3+g_6)\xi_1\omega_1 + 2(1+\mu_1)(1+g_4)\xi_d\omega_d \tag{57}$$

$$a_4 = 1 - g_5 + (1+\mu_1)g_6 \tag{58}$$

The spectral density of the generalized coordinates can be expressed as

$$[S_{YY}(\omega)] = [S_{Y_iY_j}(\omega)] = [H^*(\mathrm{i}\omega)][S_{FF}(\omega)][H(\mathrm{i}\omega)]^{\mathrm{T}} \tag{59}$$

where $[S_{FF}(\omega)]$ is a matrix of the spectral density of excitation and the superscript * denotes complex conjugate.

For wind excitation, we have

$$[S_{FF}(\omega)] = \begin{bmatrix} A_1^2 & 0 \\ 0 & 0 \end{bmatrix} S_{vv}(\omega) \tag{60}$$

where $S_{vv}(\omega)$ is the spectral density of wind speed at the reference height. Therefore, the spectral densities of $y_j$ are

$$S_{y_1y_1}(\omega) = \frac{1}{|\Delta|^2}A_1^2 h_{11}h_{11}^* S_{vv}(\omega) \tag{61}$$

$$S_{y_1y_2}(\omega) = \frac{1}{|\Delta|^2}A_1^2 h_{21}h_{11}^* S_{vv}(\omega) \tag{62}$$

$$S_{y_2y_1}(\omega) = \frac{1}{|\Delta|^2}A_1^2 h_{11}h_{21}^* S_{vv}(\omega) \tag{63}$$

$$S_{y_2y_2}(\omega) = \frac{1}{|\Delta|^2}A_1^2 h_{21}h_{21}^* S_{vv}(\omega) \tag{64}$$

The spectral density of $y_1$ can be obtained by substituting Eqs. (49)–(53) into Eq. (61) as

$$\begin{aligned} S_{y_1y_1}(\omega) &= \frac{\sum_{j=1}^{3} b_j(\omega^2)}{|\Delta|^2} \\ &= \frac{S_{vv}(\omega)}{|\Delta|^2}A_1^2\Big[(1+g_6)^2\omega^4 - 2(1+g_2) \\ &\quad\times(1+g_6)\omega_d^2\omega^2 + (1+g_2)^2\omega_d^4 \\ &\quad + 4(1+g_4)^2\xi_d^2\omega_d^2\omega^2\Big] \end{aligned} \tag{65}$$

When the excitation is white noise,

$$S_{vv}(\omega) = S_0$$

The parameters $b_j$ in Eq. (65) are, assuming $S_0 = 1$,

$$b_0 = \Lambda_1^2(1+g_2)^2\omega_d^4 \tag{66}$$

$$b_1 = -2\Lambda_1^2(1+g_2)(1+g_6)\omega_d^2 + 4\Lambda_1^2(1+g_4)^2\xi_d^2\omega_d^2 \tag{67}$$

$$b_2 = \Lambda_1^2(1+g_6)^2 \tag{68}$$

$$b_3 = 0 \tag{69}$$

The variance of $y_1$ is [15]

$$\sigma_{y_1}^2 = \frac{B_4\pi}{a_4A_4} \tag{70}$$

where

$$A_4 = a_0\left(-a_4a_1^2 + a_1a_2a_3 - a_0a_3^2\right) \tag{71}$$

$$B_4 = a_4[b_0(a_3a_2 - a_4a_1) + a_0(a_3b_1 + a_1b_2)] \tag{72}$$

The minimum variance of $y_1$ can be reached when its derivative become zero, i.e.,

$$B_4\frac{\partial A_4}{\partial g_i} - \frac{\partial B_4}{\partial g_i}A_4 = 0, \quad i = 1,2,\ldots,6 \tag{73}$$

and the optimal control gains for the ATMD can be determined from the above equation.

## 5. Simplified design method

It is difficult to derive a simplified design method for ATMD from the conventional control methods, such as the LQR method. However, a simplified design method can be deduced from the method presented above.

The equivalent damping ratio $\xi_e$ of the ATMD system, comprising the ATMD and the main structure, can be easily determined from the variance of displacement.

$$\sigma_{y_1}^2 = \frac{\Lambda_1^2\pi}{2\xi_e\omega_1^3} \tag{74}$$

Substituting Eq. (74) into Eq. (70) leads to

$$\xi_e = \frac{a_4A_4\Lambda_1^2}{2B_4\omega_1^3} \tag{75}$$

$A_4$ and $B_4$ are expressed in Eqs. (71) and (72), respectively.

It is necessary to point out that the equivalent damping ratio is a very important parameter for designing ATMD. When the equivalent damping ratio is given, one can easily evaluate the response reduction caused by the ATMD. Therefore, Eq. (75) is very useful in the design of ATMD system.

## 6. Modal decoupling

The methods proposed above are based on the assumption that only the first mode is considered in the design of ATMD systems. This assumption may be true for high-rise structures under winds. However, for many cases the higher modes can not be neglected in the design of ATMD systems for stiff buildings subjected to wind actions or structures under earthquake excitations. For these cases the above formulas must be modified.

Using the mode-superposition method results in the modal equations as follows:

$$\ddot{y}_j + 2\xi_j\omega_j\dot{y}_j + \omega_j^2y_j - \mu_j2\xi_d\omega_d\dot{x}_d - \mu_j\omega_d^2x_d = \Lambda_jv(t) - \frac{u(t)}{\widehat{M}_j}, \quad j = 1,2,\ldots,m \tag{76}$$

$$\sum_{i=1}^{m}\ddot{y}_i + \ddot{x}_d + 2\xi_d\omega_d\dot{x}_d + \omega_d^2x_d = \frac{1}{m_d}u(t) \tag{77}$$

It can be seen from the above equations that all the modal equations of the main structure expressed in Eq. (76) are independent, however, the equation of motion of the ATDM expressed in Eq. (77) is coupled with each of the first set through the summation term.

In order to simplify the analysis we assume that the movement of the ATMD and the active force can be written as

$$x_d = \sum_{i=1}^{m}x_{di} \tag{78}$$

$$u(t) = \sum_{i=1}^{m}u_i(t) \tag{79}$$

Although there is no apparent mathematical rigorous proof for verifying the assumption, numerical simulation results have shown that this simplification is sufficiently accurate [2].

Substituting Eqs. (78) and (79) into Eq. (77) leads to a set of independent equations

$$\ddot{y}_j + \ddot{x}_{dj} + 2\xi_d\omega_d\dot{x}_{dj} + \omega_d^2x_{dj} = \frac{1}{m_d}u_j(t) \tag{80}$$

The response of each mode can be analyzed independently using the following state equation of the generalized coordinate for the $j$th mode of the ATMD system, comprising the ATMD and the main structure.

$$\{\dot{Z}_j(t)\} = [A_j]\{Z_j(t)\} + \{B_j\}u_j(t) + \{F_j(t)\}v(t) \tag{81}$$

where

$$\{Z_j(t)\} = \begin{Bmatrix} y_j \\ x_{dj} \\ \dot{y}_j \\ \dot{x}_{dj} \end{Bmatrix},$$

$$[A_j] = \begin{bmatrix} 0 & 0 & 1 & 0 \\ 0 & 0 & 1 & 0 \\ -2\xi_j\omega_j & 2\mu_j\xi_d\omega_d & -\omega_j^2 & \mu_j\omega_d^2 \\ 2\xi_j\omega_j & -2(1+\mu_j)\xi_d\omega_d & \omega_j^2 & -(1+\mu_j)\omega_d^2 \end{bmatrix},$$

$$\{B_j\} = \begin{Bmatrix} 0 \\ 0 \\ -\frac{1}{\hat{M}_j} \\ \frac{1}{m_d} + \frac{1}{\hat{M}_j} \end{Bmatrix}, \quad \{F_j(t)\} = \begin{Bmatrix} 0 \\ 0 \\ \Lambda_j \\ -\Lambda_j \end{Bmatrix} \tag{82}$$

## 7. Numerical results

The design of an active mass damper for a tall (340 m) TV transmission tower in Nanjing, China was conducted by Cao et al. [2,3]. The Nanjing TV tower has two observation decks at heights of 180 and 240 m. Cao [2] showed that the acceleration response of the upper observation deck is too high and a structural control device is required to reduce the acceleration response. Consequently, an active mass damper was designed [2,3] and has been installed on the upper observation deck to reduce the acceleration response. The details of the structural systems, parameters and dynamic characteristics, etc. of the Nanjing TV tower were given by Cao et al. [2,3]. In order to examine the performance of the proposed control strategies, the Nanjing TV tower is considered in the following simulation study (Example 1 and Example 2).

*Example 1*: Table 1 shows the simulated amplitudes of the Nanjing TV tower under harmonic excitation, where the wind loading is assumed to be

$$v(t) = 2\sin\omega_1 t \tag{83}$$

The control gains listed in Table 1 are obtained from Eqs. (38) and (39) for state feedback and from Eqs. (40) and (41) for velocity feedback based on required stroke of the mass and displacement amplitude of the main structure. It can be seen from Table 1 that the present method has good accuracy as the amplitudes obtained from the present simulation are very close to the required ones. In the last four columns of Table 1, the solvable conditions given by Eqs. (34) and (35) are checked, where $B'$ and $C'$ are defined as $B' = \mu_1\omega^2 B$ and $C' = \Lambda_1 v_0$.

*Example 2*: In order to examine the effectiveness of the control strategy for controlled structure under random excitations, the wind-induced peak responses of the main structure (Nanjing TV tower) and the ATMD system without the stroke limit are calculated using the present method and LQR method. The fluctuating wind actions on this high-rise structure were simulated following the procedure given by Cao [2]. The computational results are listed in Table 2. It can be seen from Table 2 that the peak responses determined from the present method are very close to those obtained from the LQR method, while the present method result in a better reduction on acceleration responses which are of the primary concern in the design of this high-rise structure. The typical examples of time histories of responses at the upper observation deck of the Nanjing TV tower without ATMD and with ATMD are shown in Figs. 3–5 for comparison purposes.

*Example 3*: An 80-storey tall building with steel structures and ATMD system, which will be built in the south part of China, is considered herein as a numerical example to examine the performance of the proposed formulas and control strategies. The height of the building is 375 m and its plane is square with the width of 44.5 m. An ATMD system was designed and will be installed in the 71st floor.

The total mass and the first three natural frequencies (in the along-wind direction) are found as

$$M = 174,390T, \quad \omega_1 = 1.42 \quad \text{rad/s}, \quad \omega_2 = 3.14, \quad \omega_3 = 3.33$$

The damping ratio of the main structure is assumed as $\xi_i = 0.01$ ($i = 1, 2, 3$).

The mass of the ATMD is taken as 0.008 M (i.e., $\mu = 0.008$), the damping ratio is determined as 0.045 based on the following formula [11].

$$\xi_d = 0.5\sqrt{\mu} \tag{84}$$

The design wind pressure with return period of 10 years at the reference height (10 m) is determined as 0.56 kN/m$^2$ based on the Load Code for the Design of Building Structures in China. The design wind speed can be determined from the design wind pressure by the Load Code. The time history of wind action for this case is simulated following the procedure given in Cao [2]. The responses of this controlled structure under the action of wind with return period of 10 years (random excitation) are calculated.

The maximum values of acceleration at the top level of the main structure without ATMD are determined as 28.26 cm/s$^2$ (considering the first mode only) and 28.48 cm/s$^2$ (including the first three modes). The corresponding responses of the main structure with ATMD are evaluated as 12.60 cm/s$^2$ [12.66 cm/s$^2$] (considering the first mode only) and 12.91 cm/s$^2$ [12.99 cm/s$^2$] (including the first three modes). The values in bracket

Table 1
Amplitude under harmonic excitation–wind excitation

| Case | Control gain | | | | Amplitude | | $\lvert C' - B' \rvert$ | $A'$ | $\lvert C' - A' \rvert$ | $B'$ |
|---|---|---|---|---|---|---|---|---|---|---|
| | $g_3$ | $g_4$ | $g_5$ ($g_1$) | $g_6$ ($g_2$) | mass (m) | deck (m) | | | | |
| NC | 0 | 0 | 0 | 0 | 0.000 | 0.331 | | | | |
| *State velocity feedback* | | | | | | | | | | |
| Stroke $A = 1.0$ | | | | | | | | | | |
| 1 | −0.369 | 4.843 | 0.1 | −0.2 | 0.984 | 0.080 (0.08) | 0.0066 | 0.0077 | 0.0236 | 0.0247 |
| 2 | −1.630 | 7.533 | 0.1 | −0.2 | 0.977 | 0.099 (0.10) | 0.0066 | 0.0096 | 0.0216 | 0.0247 |
| 3 | −1.792 | 5.960 | 0.1 | −0.2 | 0.985 | 0.080 (0.08) | 0.0066 | 0.0077 | 0.0236 | 0.0247 |
| 4 | −3.015 | 9.933 | 0.1 | −0.2 | 0.977 | 0.098 (0.10) | 0.0066 | 0.0096 | 0.0216 | 0.0247 |
| 5 | −4.128 | 15.006 | 0.1 | −0.2 | 0.968 | 0.117 (0.12) | 0.0066 | 0.0116 | 0.0197 | 0.0247 |
| 6 | −6.050 | 25.857 | 0.1 | −0.2 | 0.950 | 0.143 (0.14) | 0.0066 | 0.0135 | 0.0178 | 0.0247 |
| Stroke $A = 1.2$ | | | | | | | | | | |
| 7 | −3.575 | 5.338 | 0.1 | 0.2 | 1.232 | 0.066 (0.06) | 0.0016 | 0.0580 | 0.0256 | 0.0297 |
| 8 | −5.933 | 10.676 | 0.1 | 0.2 | 1.269 | 0.085 (0.08) | 0.0016 | 0.0077 | 0.0236 | 0.0297 |
| Stroke $A = 0.8$ | | | | | | | | | | |
| 9 | 0.686 | 10.429 | 0.1 | −0.2 | 0.807 | 0.122 (0.12) | 0.0115 | 0.0116 | 0.0197 | 0.0198 |
| 10 | −1.004 | 12.801 | 0.1 | −0.2 | 0.759 | 0.133 (0.14) | 0.0115 | 0.0135 | 0.0178 | 0.0198 |
| *State feedback* | | | | | | | | | | |
| Stroke $A = 1.0$ | | | | | | | | | | |
| 11 | 0.154 | −0.087 | (−0.01) | (0.1) | 1.075 | 0.090 (0.08) | 0.0066 | 0.0077 | 0.0236 | 0.0247 |
| 12 | −0.087 | 0.213 | (−0.01) | (0.1) | 1.035 | 0.107 (0.10) | 0.0066 | 0.0096 | 0.0216 | 0.0247 |
| 13 | −0.286 | 0.767 | (−0.01) | (0.1) | 1.030 | 0.125 (0.12) | 0.0066 | 0.0116 | 0.0197 | 0.0247 |
| 14 | −0.604 | 2.127 | (−0.01) | (0.1) | 0.995 | 0.148 (0.14) | 0.0066 | 0.0135 | 0.0178 | 0.0247 |
| Stroke $A = 0.8$ | | | | | | | | | | |
| 15 | 0.239 | 1.182 | (−0.01) | (0.1) | 0.809 | 0.122 (0.12) | 0.0115 | 0.0116 | 0.0197 | 0.0198 |
| 16 | −0.081 | 1.353 | (−0.01) | (0.1) | 0.775 | 0.135 (0.14) | 0.0115 | 0.0135 | 0.0178 | 0.0198 |
| 17 | −0.263 | 2.034 | (−0.01) | (0.1) | 0.762 | 0.150 (0.16) | 0.0115 | 0.0154 | 0.0158 | 0.0198 |
| 18 | −0.645 | 4.518 | (−0.01) | (0.1) | 0.734 | 0.180 (0.18) | 0.0115 | 0.0174 | 0.0139 | 0.0198 |

*Note*: Amplitudes listed in Table 1 are simulated quantities and those (in parentheses) determined by the required stroke of the mass and displacement of the main structure.

Table 2
Comparison of peak response between the present method and LQR method

| Case | Displacement (m) | | | | Velocity (m/s) | | | | Acceleration (mg) | | | | Control force (kN) | |
|---|---|---|---|---|---|---|---|---|---|---|---|---|---|---|
| | PM | | LQR | | PM | | LQR | | PM | | LQR | | PM | LQR |
| | $x_d$ | $x$ | $x_d$ | $x$ | $V_d$ | $V$ | $V_d$ | $V$ | $A_d$ | $A$ | $A_d$ | $A$ | | |
| 1 | 1.101 | 0.086 | 0.0987 | 0.088 | 1.685 | 0.081 | 1.564 | 0.085 | 293.4 | 13.4 | 285.4 | 14.2 | 160.0 | 163.7 |
| 2 | 1.123 | 0.086 | 1.120 | 0.087 | 1.703 | 0.082 | 1.619 | 0.084 | 296.3 | 13.3 | 291.3 | 14.0 | 168.4 | 172.4 |
| 3 | 1.172 | 0.086 | 1.171 | 0.85 | 1.756 | 0.083 | 1.743 | 0.083 | 301.2 | 13.2 | 294.1 | 13.7 | 186.8 | 190.3 |
| 4 | 1.210 | 0.086 | 1.214 | 0.085 | 1.901 | 0.084 | 1.868 | 0.083 | 343.1 | 13.3 | 323.7 | 13.7 | 206.5 | 207.1 |

*Note:* (1) PM represents the present method; (2) $x_d$, $V_d$, $A_d$ and $x$, $V$, $A$ are the simulated displacement, velocity, acceleration of the ATMD and the main structure, respectively.

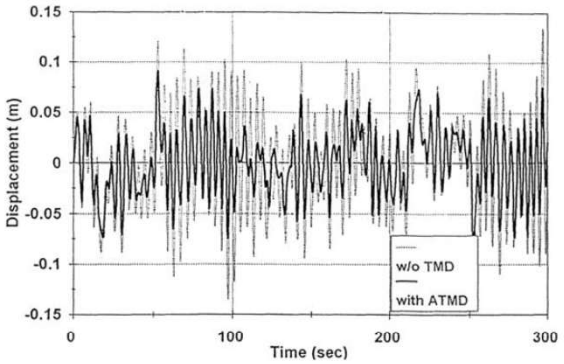


Fig. 3. Simulated observation deck displacement (state feedback control).

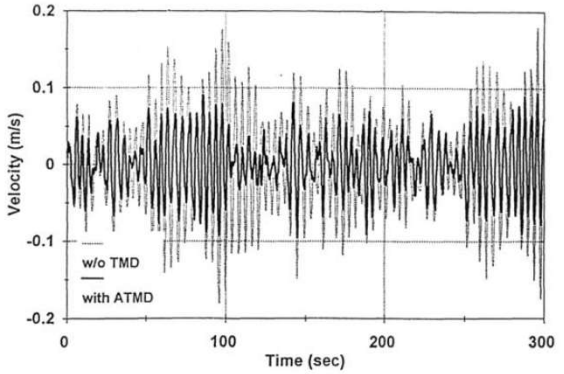


Fig. 4. Simulated observation deck velocity (state feedback control).

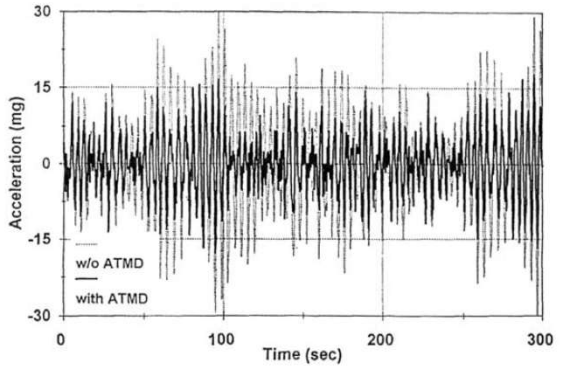


Fig. 5. Simulated observation deck acceleration (state feedback control).

parentheses are calculated by using the LQR method, which are presented herein for comparison purposes.

Using the simplified design formula, Eq. (75), we obtain $\xi_e = 0.05482$. The main structure and the ATMD system are then modeled as a multi-degree of freedom (MDOF) system. The responses of the MDOF system

can be easily evaluated by conventional structural dynamic analysis. The maximum values of acceleration responses at the top level of the main structure are determined as 13.05 cm/s$^2$ (considering the first mode only) and 13.69 cm/s$^2$ (including the first three modes).

It can be seen from the above results that the effect of higher modes on the acceleration of the main structure under winds is not significant, and the results determined from the present method are very close to those obtained from the LQR method. But the present method has a better reduction on acceleration responses.

It is also shown that the results obtained from the simplified design method are in good agreement with those determined from the present method and the LQR method.

It should be mentioned that the computational time required by the present method is less than that needed by the LQR method.

## 8. Conclusions

The active tuned mass dampers have many advantages, such as high efficiency and flexibility. In this paper, a different structural control approach is developed. Instead of solving the Riccati equation, new control strategies are developed from a response parameter analysis and based on the linear feedback control for the design of ATMD systems under dynamic excitations. Based on the proposed strategies, a simplified method for ATMD design is presented. The equivalent damping induced by an ATMD can be easily determined by the simplified method. When the equivalent damping ratio is given, one can easily evaluate the response reduction caused by the ATMD. The numerical examples show that the present strategies result in a better reduction on acceleration response than the LQR method. It is also shown through a numerical example that the results determined from the simplified design method are in good agreement with those obtained from the present strategies and the LQR method. Therefore, the proposed strategies and method are applicable in structural control implementation.

## Acknowledgements

Valuable suggestions and comments provided by Prof. T.T. Soong and Prof. A.M. Reinhorn of SUNY, Buffalo for this study are gratefully acknowledged. The work described in this paper was partially supported by a grant from Research Grant Council of Hong Kong Special Administrative Region, China (project no. CityU 1131/00E).

## References

[1] Abdel-rohman M. Effectiveness of active TMD for building control. Trans Can Soc Mech Engrs 1984;8:179–84.
[2] Cao H. Analysis and design of active tuned mass damper systems. Ph.D. Dissertation. State University of New York at Buffalo, 1997.
[3] Cao H, Reinhorn AM, Soong TT. Design of an active mass damper for wind response of Nanjing TV tower. Eng Struct 1998;20:134–43.
[4] Chang JCH, Soong TT. Structural control using active tuned mass dampers. J Eng Mech, ASCE 1980;106:1091–8.
[5] Higashino M, Aizawa S. The application of active mass damper system in actual buildings. Report of Research & Development Institute. Takenaka Corporation, 1994.
[6] Hrovat D, Barak P, Robins M. Semi-active vs passive or active tuned mass dampers for structural control. J Eng Mech, ASCE 1983;109:691–901.
[7] Kobori T, Koshika N, Yamada K, Ikeda Y. Seismic-response-controlled structure with active mass driver system. Part 1: design. Earthquake Eng Struct Dynam 1991;20:133–49.
[8] Kobori T, Koshika N, Yamada K, Ikeda Y. Seismic-response-controlled structure with active mass driver system. Part 2: verification. Earthquake Eng Struct Dynam 1991;20:151–66.
[9] Li QS, Cao H, Li GQ. Analysis of free vibrations of tall buildings. J Eng Mech, ASCE 1994;120:1861–76.
[10] Li QS, Fang JQ, Jeary AP, Wong CK. Full scale measurements of wind effects on tall buildings. J Wind Eng Ind Aerodynam 1998;74-76:741–50.
[11] Li QS, Cao H, Li GQ, Li SJ, Liu DK. Optimal design of wind-induced vibration control of tall buildings and high-rise structures. Wind Struct 1999;2(1):69–83.
[12] Lund RA. Active damping of large structures. In: Leipholz HHE, editor. Winds structural control. Amsterdam: North-Holland; 1980. p. 459–70.
[13] Soong TT. Active structural control: theory and practice. New York: John Wiley & Sons; 1990. p. 136–46.
[14] Reinhorn AM, Manolis GD. Recent advances in structural control. Shock Vibrat Digest 1989;21:3–8.
[15] Roberts JR, Spanos PD. Random vibration and statistical linearization. New York: John Wiley & Sons; 1990.
[16] Rodellar J, Chung LL, Soong TT, Reinhorn AM. Experimental digital predictive control of structures. J Eng Mech, ASCE 1989;115:1245–61.